



Libraries and Learning Services

# University of Auckland Research Repository, ResearchSpace

## Version

This is the Accepted Manuscript version of the following article. This version is defined in the NISO recommended practice RP-8-2008

<http://www.niso.org/publications/rp/>

## Suggested Reference

Yang, S.W., Watkinson, P., Gillies, G., & James, B. J. (2016). Microstructural transformations in anisotropy and melt-stretch properties of low moisture part skim mozzarella cheese. *International Dairy Journal*, 62, 19-27.

doi: [10.1016/j.idairyj.2016.06.013](https://doi.org/10.1016/j.idairyj.2016.06.013)

## Copyright

Items in ResearchSpace are protected by copyright, with all rights reserved, unless otherwise indicated. Previously published items are made available in accordance with the copyright policy of the publisher.

This is an open-access article distributed under the terms of the [Creative Commons Attribution-NonCommercial-NoDerivatives](https://creativecommons.org/licenses/by-nc-nd/4.0/) License.

For more information, see [General copyright](#), [Publisher copyright](#), [SHERPA/RoMEO](#).

# **Microstructural transformations in anisotropy and melt-stretch properties of low moisture part skim mozzarella cheese**

Seo Won Yang<sup>a</sup>, Philip Watkinson<sup>b</sup>, Graeme Gillies<sup>b</sup>, Bryony J. James<sup>a</sup>

<sup>a</sup>Department of Chemical and Materials Engineering, University of Auckland, Auckland, New Zealand

<sup>b</sup>Research and Development Centre, Fonterra Co-operative Group Limited, Palmerston North, New Zealand

## **Abstract**

Mozzarella cheese is primarily consumed in its melted form due to its desirable melt and stretch characteristics when heated. Understanding the relationship between the anisotropic structure and melt-stretch properties is critical for controlling functionality. A novel *ex situ* sample extraction system was developed to produce melted and stretched mozzarella. New structure analytics were established to reveal transient changes during deformation of mozzarella under dynamic heat-shear conditions. Transformations in anisotropy were examined using various microscopy techniques coupled with image analysis. Coalescence of milk fat aggregates into large droplets upon heating caused loss of anisotropy. However, fat droplets broke down into channels on stretching, comprising agglomerates of smaller droplets and anisotropy was regained. When stretched further adhesion between the agglomerated fat droplets was broken by the forces exerted from the contracted protein fibres. Large fat droplets are necessary as they act as shock absorbers that enable protein fibres to become pliable; allowing greater stretch.

## 24 1.0 Introduction

25 Mozzarella cheese is a widely used ingredient in both home cooking and food services  
26 sector. Mozzarella production is growing, in 2015 in the US alone it represented (at  $1.8 \times$   
27  $10^6$  kg) the largest volume cheese sold to restaurants, accounting for 29% of total cheese  
28 usage (largely driven by demand for pizza). (Dequaine, 2016) Consumers' perception of  
29 mozzarella is dominated by its desirable melt, stretch and stringy characteristics that emerge  
30 upon heating. These signature textural attributes are classified as functional properties  
31 (Gunasekaran & Ak, 2003) and are frequently attributed to the *pasta-filata* structure  
32 (McMahon & Oberg, 1999).

33 The *pasta-filata* microstructure in the final mozzarella product originates from the critical  
34 stretcher-cooker process during manufacture (Kindstedt & Guo, 1997; McMahon, Oberg &  
35 McManus, 1993;). The structure is heterogeneous and anisotropic combination of networks  
36 of long parallel aligned *para*-casein fibres, with elongated channels of fat oriented in the  
37 direction of stretch (Everett & Auty, 2008; Kindstedt, 2004; Kindstedt & Guo, 1997; McMahon  
38 & Oberg, 1999). Cheese manufacturers aim to produce mozzarella with structures that  
39 deliver the physical functional properties specified by the end-user (Kindstedt & Guo, 1997;  
40 McMahon *et al.*, 1993). By quantifying the link between structure and property,  
41 manufacturers can design and fabricate products using a more methodical and controlled  
42 basis (McClements, 2007).

43 Meltability and stretchability are the key functional properties that emerge on baking of  
44 mozzarella and are perceived as the signature attractive characteristic of this cheese (Chen,  
45 Wolle & Sommer, 2009; Guinee, Feeney, Auty & Fox, 2002; Rowney, Roupas, Hickey &  
46 Everett, 1999). Whilst these properties are frequently attributed to the anisotropic  
47 microstructure little attention has been paid to the transformation of that structure during  
48 melting.

49 Meltability is defined as the ability of the cheese structure to flow and form a uniform  
50 continuous melt upon heating, and it is the first point of major alteration in the structure  
51 during cooking (Kindstedt, Carlc & Milanovic, 2004; Rowney, Roupas, Hickey & Everett,  
52 1998). As the mozzarella is heated, aggregates of milk fat globules between the protein  
53 fibres liquefy at 40 °C (Joshi, Muthukumarappan & Dave, 2004; Lopez, Camier & Gassi ,  
54 2007). The liquid fats coalesce and enhance the meltability by lubricating the surfaces of  
55 adjacent para-casein network to facilitate displacement of adjoining layers of the protein  
56 matrix and effectively increase cheese flow (Kindstedt, 1993; Lucey, Johnson & Horne,  
57 2003). However, there is currently a lack of structural information on *melted* mozzarella.

58 Stretchability is known to be one of the most significant functional properties of mozzarella,  
59 yet it is the most difficult aspect to measure (Fife, McMahon & Oberg, 2002). Stretchability is  
60 defined as the capacity of melted cheese to form fibrous strands that extend without  
61 breaking under tension (Rowney *et al.*, 1999). Lucey *et al.* (2003) have provided a more  
62 precise definition; stretch is the ability of the casein network to maintain its integrity when a  
63 continuous stress is applied to the cheese.

64 Many authors (Ak, Bogenrief, Gunaskaran & Olsen, 1993; Ak & Gunasekaran, 1995;  
65 Apostopoulos, 1993; Cavella, Chemin & Masi, 1992; Fife *et al.*, 2002; Ma, James, Zhang &  
66 Emanuelsson-Patterson, 2012; Wang, Muthukumarappan, Ak & Gunasekaran., 1998) have  
67 implemented objective stretch tests that provides quantitative rheological measurements of  
68 the cheese stretched under controlled environmental conditions. However, even with the  
69 possibility of quantifying stretch, the *mechanism* of stretch still remains unclear as to how the  
70 microstructure deforms.

71 One difficulty in directly visualising the effect of heat on the microstructure of mozzarella  
72 arises from the difficulty in handling soft mozzarella because of its viscoelastic behaviour.  
73 As strained materials are sampled stress relaxation immediately alters the structure. Simply  
74 put, cutting a sample from stretched cheese alters the microstructure before analysis.

Thus, designing a method to extract the strained structure with the loading orientation and strained microstructure intact is critical to producing samples for microstructural analysis. The purpose of the current study was to reveal changes in microstructure on melting and stretching in order to quantify their role in mechanism of melt flow and stretchability. Melted and stretched mozzarella samples were produced using a sampling system capable of extracting samples with the loading orientation and the strained microstructure intact. These samples were then analysed using advanced complementary microscopy techniques combined with image analysis to quantify key structural parameters in the mozzarella microstructure under controlled heat-shear conditions.

## 2.0 Materials and methods

Low moisture, part-skim mozzarella samples (Galaxy Mozzarella Cheese, Fonterra Brands Ltd., Auckland New Zealand) were purchased as 200 g blocks from a local supermarket. The composition of the mozzarella was: 19.9 g fat per 100 g cheese, 26.7 g protein per 100 g cheese, 50.9 g water per 100 g cheese and 0.5 g salt per 100 g cheese. The mozzarella was reported to be packed at the age of approximately 4 to 8 wk, vacuum sealed and stored at 2 °C.

### 2.1 Sample extraction system

A sample extraction system was designed and fabricated based on modifications of Ma *et al.*'s (2012) stretching apparatus to produce melted and stretched mozzarella to capture in-built strain in the structure, and to arrest the deformation of fat during melting and stretching for microstructure characterisation.

A 10 g sample of mozzarella was placed into a stainless steel tube and covered with aluminium foil to prevent dehydration. The tube and cheese was then heated in a hot water bath at 75 °C for 15 min to achieve a melt temperature of 70 °C. After heating a Teflon sleeve (which was also heated in the same water bath) was slid onto the tube to insulate and reduce the change in temperature of the sample. A 3-prong hook attached to the Instron crosshead was lowered into the pool of mozzarella, 5mm above the rig base, as shown in Fig. 1a.

The hook was subsequently rotated clockwise by 90° and locked into position. The mozzarella was pulled vertically at 1000 mm.min<sup>-1</sup>. The strained structure was immediately frozen in place by pouring liquid N<sub>2</sub> into the rig as illustrated in Fig. 1b. Removing the sample from the rig prior to freezing could not be accomplished without further deformation of the sample. As such quenching the stretched mozzarella using liquid nitrogen was found to be the most effective method of preserving the strained microstructure & arresting the transient deformations. Instantaneous solidification prevented further deformation from gravity and minimised artefacts during handling of samples that were in a viscous or malleable state.

The mozzarella sample was taken (Fig. 1c) from the centre of the stretched sample. Extracted samples were placed inside an airtight container and immediately stored at -20 °C in a freezer. Samples were taken at stretched lengths of 50 mm, 100 mm and 150 mm, giving strains of 280 %, 580 % and 900 % respectively at a strain rate of about 10 s<sup>-1</sup>. Unstretched samples were also taken by melting the cheese using the steps above, freezing then unsealing the tube.

## 2.2 Microstructure characterisation

Confocal laser scanning microscopy (CLSM), environmental scanning electron microscopy (ESEM) and cryo-SEM were used to observe the microstructure of the unmelted, melted and strained mozzarella. This set of microscopy techniques were selected as they accommodate the inspection of fully hydrated samples, use mild or no sample preparation and less inclined to introduce artefacts (James, 2009).

### 2.2.1 Confocal laser scanning microscopy

CLSM was used to observe the change in fat size and shape of fat globules and channels within the protein matrix for unmelted, melted, and melted and stretched mozzarella. Samples, previously stored at -20 °C as described above, were cut to 10 mm×10 mm×10 mm. Specimens were cryo-sectioned to thickness of 50 µm along the longitudinal axis at -20 °C using a cryostat (Leica CM1850 Cryomicrotome, Buffalo Grove, IL, USA).

The sectioned specimens were placed onto flat glass microscope slides. Two drops of Nile red/FCF fast green stain (Sigma-Aldrich, St. Louis, MO, USA) were applied to the coverslip using a pipette and placed onto the specimen. The stain was composed of 0.5 % Nile red and 0.2 % fast green FCF dyes diluted in AF1 Citifluor (a glycerol-PBS solution containing an amine antifadeant) (Sigma-Aldrich, St. Louis, MO, USA). The prepared slides were placed in a light-proof container to prevent photo bleaching and left to stain overnight in a refrigerator at 4 °C.

Confocal micrographs were taken using a 40× magnification oil immersion lens (Leica TCS SP2, Buffalo Grove, IL, USA: objective lens specifications HCX Plan Apo 40X/1.25 oil with numerical aperture 1.25). An He/Ne laser with a wavelength of 633 nm was used to excite the Nile red dye and emissions were collected at 575-600 nm for the fat phase. Kr/Ar laser with a wavelength of 488 nm was used to excite the fast green and emissions were collected

above 645 nm for the protein phase. Images consisting of 512 × 512 pixels were acquired at approximately 20 to 25 µm below the sample surface using a line average of 8.

### 2.2.2 Environmental scanning electron microscopy

ESEM was conducted to investigate the microstructure of mozzarella in its native state at a high resolution. The internal structure of the unmelted, melted and stretched mozzarella samples were examined. The internal microstructure was revealed by thawing the samples at room temperature for 1 min and peeling along the fibre direction. The peeled section was cut into a rectangular section to a dimension of 4 mm by 4 mm (length, width) by 1 mm thickness. The peeled surface (not the cut edges) was viewed.

Scanning electron microscopy was conducted in an environmental scanning electron microscope equipped with a peltier cooling stage (Quanta 200F SEM, FEI, Eindhoven, The Netherlands). Water vapour was used as the imaging gas and the sample chamber was pumped through five cycles (minimum pressure of 430 Nm<sup>-2</sup> and maximum of pressure 930 Nm<sup>-2</sup> Torr) to stabilise the water vapour pressure. An accelerating voltage of 10 kV and working distance of approximately 5 mm-6 mm was used. Pressure of 430 Nm<sup>-2</sup> Torr and temperature of 2.0 °C was used to establish a relative humidity of 60 % during imaging.

### 2.2.3 Cryogenic scanning electron microscopy

Cryo-SEM was also used to observe the internal structure of the cheese. Samples were cut into sections with a height of 4 mm, length of 3 mm and width of 1 to 2 mm and mounted onto a copper sample holder. The copper holder, with mounted specimen, was plunged into liquid N<sub>2</sub> slush at -210 °C. The frozen specimens were transferred under vacuum conditions to the preparation chamber (Alto 2500 cryo-trans system, Gatan, Pleasanton, CA, USA)



where they were cryo-fractured with a scalpel blade at -187 °C. The specimens were subsequently allowed to warm to -90 °C for 30 min to sublime water, cooled again and sputter coated with gold. The specimen was transferred onto a liquid nitrogen cooled cold-stage module, maintained at -187 °C and observed using a field emission scanning electron microscope (XL30 S-FEG, FEI/Philips, Eindhoven, The Netherlands). Images were captured with an accelerating voltage of 5 kV using a secondary electron detector. Cryo-SEM was not carried out for 100 mm and 150 mm stretched mozzarella due to the restriction of the sample geometry as these samples were too thin to handle easily for freeze-fracture, as the sample needs to be held in the sample holder, frozen then fractured in the sample preparation chamber of the cryo-transfer system.

#### 2.2.4 Quantification of fat channels

CLSM images only containing the fat channels (obtained from 488 nm excitation) were selected for quantification using LensEye software (Engineering & Cyber Solutions, Gainesville, FL, U.S.A.). The fat channels were segmented by manually applying a binary threshold to the image. For the fat analysis, objects in contact with the edges of the image were removed. Eight images were analysed in terms of area, aspect ratio and spatial distribution for each unmelted, melted, and melted and stretched sample. Statistical treatment of the measurements was conducted by extracting a mean and 95 % confidence interval based on the number of “objects” identified. Across 8 images there were between 900 and 1300 objects included for these measurements.

Area (of fat channels) was measured by calculating the area of the segmented fat channels in pixels. The area in pixels was converted into micrometre squared. The aspect ratio was used to describe and quantify the shape of fat channels, more specifically magnitude of elongation corresponding to its unmelted, melted and strained conditions. Aspect ratio was

calculated by dividing the longest length by the shortest length of the fat channel or globule. An aspect ratio of one indicates a perfectly circular fat particle and increases as the fat elongates.

The spatial distribution of fat was quantified by measuring the minimum neighbouring distance between each individual fat channel. This function was employed to estimate the dispersion of fat in the protein matrix and the degree of fat emulsification in mozzarella. The minimum distance between the fat was measured by searching for the nearest fat from each particle count and measuring the distance (shown with an arrow, Fig. 2) between the centres of gravity (shown with a circular dot, Fig. 2, and defined as the the average x- and y-positions of a binary object) of each fat channel.

#### 2.2.5 Quantification of fat droplets

ESEM images revealed that the fat “channels” observed in CLSM were comprised of aligned aggregates of spherical milk fat globules. Segmentation of SEM images is difficult due to the large variation of grey tones in the micrographs. In addition, artefacts can be introduced from using various filters from conventional image processing software. In this case, higher precision was obtained from manual segmentation of objects, rather than automated procedures. Therefore, manual segmentation was employed for fat droplet quantification by drawing super-imposed lines in Image Pro Premier (Mediacybernetics, Rockville, MD, USA) along the major axis of each individual fat droplet in the ESEM images. Statistical treatment of the measurements was conducted by extracting a mean and 95% confidence interval based on the number of objects (ie fat droplets) identified. At the higher magnification of ESEM a lower number of individual “objects” can be identified and between 100 and 500 objects across, up to 50 images were included for these measurements.

220

## 221 3.0 Results

222 Changes were observed and measured in the strained samples indicating heat and strain  
223 induced changes in anisotropy and microstructure of the fat channels and the fat droplets  
224 within those channels. Fat channels and fat droplets were assessed separately.

225

## 226 3.1 Microstructure observation and evaluation

### 227 3.1.2 Fat channels

228 Fig. 3 shows CLSM images showing the longitudinal fibre axis of unmelted, melted and  
229 melted and stretched mozzarella. As expected unmelted mozzarella showed elongated fat  
230 channels in the protein matrix, forming a highly anisotropic structure (Everett & Auty 2008).

231 Heating to 70 °C induced complete loss of detectable structural anisotropy as the elongated  
232 fat channels coalesced to form large spherical fat droplets with relaxation of the protein  
233 matrix. These spherical fat droplets existed in a wide range of sizes, from less than 10 µm to  
234 up to as large as 200 µm in diameter. These large droplets elongated in the direction of  
235 strain when the mozzarella was stretched, and began to break up when the strain increased.

236

### 237 3.2.2 Fat droplets

238 The fractured longitudinal sections of the unmelted, melted and melted and stretched  
239 mozzarella were examined using the ESEM to show the morphology of the fat droplets  
240 within the channels, shown in Fig. 4. The fat channels in unmelted mozzarella were  
241 comprised of aggregates of milk fat globules with diameters ranging from 1 to 15 µm,  
242 consistent with previous studies (Kuo & Gunasekaran, 2009). Similar to the observations

made in the confocal micrographs, heating resulted in a loss of anisotropy, with coalescence of milk fat globules forming large fat droplets up to 200  $\mu\text{m}$  in diameter.

When a stretch yielding a strain of 280% was applied, the large droplets broke down into bundles of smaller agglomerated droplets and, with additional strain, anisotropy was regained as protein “fibres” reappeared as fat droplets broke up and channels of fat droplets became aligned in the direction of strain. The fat droplets showed distinct striations on the droplet surface indicating that the protein fibres were exerting stress perpendicular to the stretch direction during strain. Furthermore, the protein strand striation marks also indicated that protein phase possesses a relatively higher stiffness than the fat phase. This is in line with other studies that have suggested values of Young’s modulus for dairy protein fibrils in the order of a few  $\text{GNm}^{-2}$  (Pan & Zhong, 2015), whereas fat networks have values in the order of a few  $\text{MNm}^{-2}$  (Maleky, Campos & Marangoni, 2007).

The degree of heterogeneity and anisotropy increased in the structure as the agglomerated droplets broke down to smaller diameters. Cryo-SEM showed similar morphology to ESEM analysis (Fig. 5).

## 3.2 Image analysis

### 3.2.1 Quantification of fat channels

The size of the fat channels in the samples was estimated by measuring the mean area of each channel, Fig. 6. The mean size of fat channels in the melted state ( $419 \pm 267 \mu\text{m}^2$ ) was considerably larger than that in the unmelted state ( $179 \pm 74 \mu\text{m}^2$ ). This suggests that melting allowed the coalescence of droplets from more than one visible channel, since the channels have a 3-dimensional structure this is likely a result of a single channel, with out of plane branches, collapsing to a single droplet. The fat channel area started to decrease as strain

was applied, levelling out after a stretch by 580 % strain. The aspect ratio of the fat channels also indicates this coalescence into larger, more spherical drops as shown in Fig. 7.

Fig. 8 shows that minimum neighbouring distance was the lowest ( $13.0 \pm 0.4 \mu\text{m}$ ) in the unmelted mozzarella. The stretcher cooker results in a uniform distribution of narrow fat channels, which, on melting and reforming under strain form fewer, fat channels more widely spaced.

### 3.2.2 Quantification of fat droplets

The mean fat droplet diameter is plotted in Fig. 9. The fat channels observed in CLSM (Fig. 3) were comprised of these fat droplets apparent in ESEM (Fig. 4). The milk fat globules within the aggregates were the smallest in the unmelted state ( $4.2 \pm 0.2 \mu\text{m}$ ) at 4 °C and the fat globule sizes were representative of the range of sizes found in raw milk and cheese (Walstra, Wouters & Geurts, 2006). Upon heating the mozzarella, the aggregated milk fat globules coalesced into large fat droplets ( $120 \pm 33 \mu\text{m}$ ), which was up to 27 times larger in size. When strain was applied, the large spherical fat globules broke down into agglomerates of smaller spherical globules, the diameter decreasing with increasing strain.

## 4.0 Discussion

### 4.1 Heat/strain induced transformations in anisotropy

The sample extraction system successfully arrested the deformation of fat during heating and stretching whilst keeping intact the loading orientation and the strained microstructure. Transformations in anisotropy were observed upon heating and stretching. Fig. 10 depicts the overall change in structure after melting and distribution of forces in the protein matrix when subjected to stretch.

291 Unmelted mozzarella possessed an anisotropic structure, with parallel aligned channels of  
292 partially solid milk fat globule aggregates between protein strands. This anisotropic  
293 structure disappears on melting at 70 °C, where the mozzarella completely lost its  
294 characteristic *pasta-filata* structure, and resembled a homogeneous curd structure, with  
295 isolated large fat droplets (Fig. 5b). During heating, the protein matrix relaxed and the  
296 partially solid fat became fully liquefied (Gunasekaran & Ak, 2003). Once sufficiently  
297 liquefied, the interfacial tension dominates and causes aggregated milk fat globules to form  
298 fewer larger droplets.

299 The origin of the large fat globules is the coalescence of fat droplets from within channels  
300 that branch outside the plane of view of the CLSM technique. Formation of large fat  
301 droplets in melted mozzarella is crucial in order to facilitate a longer stretch. These large fat  
302 droplets act as “shock absorbers” when tensile stress is applied to the melted pool of  
303 mozzarella; enabling it to stretch. Fat droplets do not adhere to the protein matrix but are  
304 contained in slightly larger domains, predominately made of water (Kinstedt & Guo, 1997;  
305 McMahon & Oberg, 1999). These fat filled water domains deform with the stretching protein  
306 matrix. In the short stretching time little viscous dissipation is expected and the local strain  
307 rate resembles the bulk strain rate. Nonetheless, the stress transmitted to the fat droplet via  
308 the elongating water domain will not deform the fat droplet. The elongational stress  
309 transmitted across the water phase ( $\eta \sim 1 \text{ mNm}^{-2}.\text{s}$ ) is the product of the viscosity and the  
310 local strain rate and of the order of  $10^{-2} \text{ Nm}^{-2}$ . This stress is insignificant compared to the  
311 smallest plausible Laplace pressure of  $10^3 \text{ Nm}^{-2}$  that assumes  $r \sim 100 \text{ }\mu\text{m}$  and a  
312 conservatively low interfacial tension of 10 mN/m. Thus the deformation arises from the  
313 compression stress generated perpendicular to the stretch direction and is carried by the  
314 protein matrix, as illustrated schematically in Fig. 10. These compressive stresses facilitate  
315 deformation of fat while the elongated serum channel restricts its shape. After sufficient  
316 droplet deformation the Laplace pressure favours the formation of multiple smaller droplets.

317 Smaller droplets deform less under the same load, and thus droplet break up will stop once  
318 droplets reach a critical size where deformation resulting in break up is no longer achievable.

319 The sample extraction system developed for this study has successfully arrested transient  
320 deformations in fat structure in viscoelastic cheese under heat-strain conditions.. This has  
321 provided understanding of the mechanism of fat deformation and redistribution during  
322 stretching.

323

#### 324 4.2 Evaluation of mozzarella structure using complementary microscopy techniques

325 The microstructure of mozzarella was explored using CLSM, ESEM and cryo-SEM. It is  
326 useful to consider the complementary information offered by each technique. Optical  
327 sectioning in CLSM permits image capture across a plane at different depths in the sample.  
328 Thus, most of the fat and protein are captured across the image plane and a representative  
329 sample for image analysis can be attained (Fig. 11a).

330 In ESEM, the topography of the observed surface is captured (Aguilera & Stanley, 1999).  
331 Therefore any fat buried underneath the protein matrix (indicated by the red circle in Fig. 11b)  
332 cannot be directly observed, until the sample is physically altered outside of the microscope.  
333 Nevertheless, ESEM offered the benefit of higher resolution when examining the milk fat  
334 globule microstructure of mozzarella. In the unmelted mozzarella, ESEM was able to reveal  
335 the morphology of individual milk fat globules in aggregates in unmelted mozzarella and  
336 clearly defined morphological outlines of the individual fat droplets within the fat channels in  
337 the stretched mozzarella (Fig. 4).

338 Cryo-SEM was also able to reveal the individual milk fat globules, the advantage of this  
339 technique is that fracture plane can bisect fat globules potentially revealing more about their  
340 interactions than ESEM. Cryo-SEM was able to reveal aggregates of the *para*-casein  
341 network that lie within the protein matrix (Fig. 5c). Sublimation of water in the fractured

sample surface exposed porosity within the protein matrix. The pores are highly likely to be the entrapped water surrounded by casein aggregates.

## 5.0 Conclusion

This significance of this study lies in the technique developed to sample melted and stretched cheese and analyse the structural components of relevance. In particular the *ex situ* sample extraction system for arresting coalescence and deformation of fat droplets as revealed that anisotropy was lost when mozzarella was fully melted and regained in the direction of applied strain when stretched.

Fat structuring is critical for developing the necessary functional properties in mozzarella. The interconnected fat channels allow the formation of large fat droplet fillers when heated which subsequently deform and facilitate stretch.

The advantage of using complementary microscopy techniques for microstructure characterisation was demonstrated by evaluating the mozzarella structure using CLSM, ESEM and cryo-SEM. CLSM, was ideal for quantifying fat channel dimensions whereas the EM techniques were well suited to examining individual fat globules and structuring in the protein matrix. Application of the sampling and structural analytics presented in this paper could lead to improved understanding of dynamic changes in cheese processing technologies. Such understanding can be used in manufacture and provide a guide for tailoring the cheese structure to produce desirable functional properties.



365 Acknowledgements

366 This work was funded by the Primary Growth Partnership (PGP) program, “Transforming the  
367 Dairy Value Chain”, funded by Fonterra Co-operative group and the NZ Ministry for Primary  
368 Industries (MPI). The authors would like to thank the Research Centre for Surface and  
369 Materials Science (RCSMS) and the Biomedical Imaging Research Unit (BIRU) at the  
370 University of Auckland, for access to equipment.

371

372

373

374 References

- 375 Aguilera, J. M. & Stanley, D. W. 1999. *Microstructural Principles of Food Processing and*  
376 *Engineering*. Maryland, USA: Aspen Publishers Inc.
- 377 Ak, M. M., Bogenrief, D., Gunasekaran, S. & Olson, N. F. 1993. Rheological evaluation of  
378 Mozzarella cheese by uniaxial horizontal extension. *Journal of Texture Studies*. 24 437-453.
- 379 Ak, M. M. & Gunasekaran, S. 1995. Measuring elongational properties of Mozzarella cheese.  
380 *Journal of Texture Studies*. 26 147-160.
- 381 Apostopoulos, C. 1993. Simple empirical and fundamental methods to determine objectively  
382 the stretchability of Mozzarella cheese. *Journal of Dairy Research*. 61 405-413.
- 383 Cavella, S., Chemin, S. & Masi, P. 1992. Objective Measurement of the stretchability of  
384 Mozzarella cheese. *Journal of Texture Studies*. 23 185-194.
- 385 Dequaine, C (March 2016) Top pizza topping Mozzarella still is increasing in demand -  
386 Retrieved from <http://www.cheesemarketnews.com/articlearch/cheese/04mar16.html>,  
387 *retrieved 25 May 2016*
- 388 Chen, C., Wolle, D. & Sommer, D. 2009. Mozzarella. In Clark, S., Costello, M., Drake, M.,  
389 Bodyfelt, F. (Eds.). *The sensory evaluation of dairy products* (pp. 459-487). New York, USA:  
390 Springer Science.
- 391 Everett, D. W. & Auty, M.A.E. 2008 Cheese structure and current methods of analysis  
392 *International Dairy Journal* 18 (7), pp. 759-773
- 393 Fife, R. L., McMahon, D. J. & Oberg, C. J. 2002. Test for measuring the stretchability of  
394 melted cheese. *Journal of Dairy Science*. 85 3539-3545.

395 Guinee, T. P., Feeney, E. P., Auty, M. A. E. & Fox, P. F. 2002. Effect of pH and calcium  
 396 concentration on some textural and functional properties of Mozzarella cheese. *Journal of*  
 397 *Dairy Science*. 85 1655-1669.

398 Gunasekaran, S. & Ak, M. 2003. *Cheese Rheology and Texture*. Boca Raton: CRC Press.

399 James, B. J. 2009. Advances in “wet” electron microscopy techniques and their application  
 400 to the study of food structure. *Trends in Food Science and Technology*. 20 114-124.

401 Joshi, N. S., Muthukumarappan, K. & Dave, R. I. 2004. Effect of calcium on microstructure  
 402 and meltability of part skim Mozzarella cheese. *Journal of Dairy Science*. 87 1975-1985.

403 Kindstedt, P. S. 1993. Effect of manufacturing factors, composition, and proteolysis on the  
 404 functional characteristics of Mozzarella cheese. *Critical Reviews in Food Science and*  
 405 *Nutrition*. 33 2 167-187.

406 Kindstedt, P. S. 2004. Mozzarella cheese: 40 years of scientific advancement. *International*  
 407 *Journal of Dairy Science*. 57 2/3 85-90.

408 Kindstedt, P.S. ,Carlc, M. & Milanovic, S. 2004. Pasta-Filata Cheeses. In *Cheese: Chemistry,*  
 409 *Physics and Microbiology*, Third Edition –Volume 2: Major Cheese Groups. 251-263.  
 410 Amsterdam, London: Elsevier.

411 Kindstedt, P. S. & Guo, M. R. 1997. Recent developments in the science and technology of  
 412 pizza cheese. *Australian Journal of Dairy Technology*. 52 41-43.

413 Kuo, M. & Gunasekaran, S. 2009. Effect of freezing and frozen storage on microstructure of  
 414 Mozzarella and pizza cheeses. *LWT – Food Science and Technology*. 42 9-16.

415 Lopez, C., Camier, B. & Gassi, J. 2007. Development of the milkfat microstructure during the  
 416 manufacture and ripening of Emmental cheese observed by confocal laser scanning  
 417 microscopy. *International Dairy Journal* 17 235-247.

418 Lucey, J.A., Johnson, M. E. & Horne, D. S. 2003. Perspectives on the basis of rheology and  
 419 texture properties of cheese. *Journal of Dairy Science*. 86 2725-2743.

420 Ma, X., James, B., Zhang, L. & Emanuelsson-Patterson, E. A. C. 2012. Stretchability test for  
 421 Mozzarella cheese. *Journal of Dairy Science*. 95 10 5561-5568.

422 Maleky, F., Campos, R. & Marangoni, A.G. 2007 Structural and Mechanical Properties of  
 423 Fats Quantified by Ultrasonics. *Journal of the American Oil Chemist's Society* 84 331-  
 424 338McClements, J. D. 2007. *Understanding and controlling the microstructure of complex*  
 425 *foods*. Cambridge, England: Woodhead Publishing Ltd.

426 McMahon, D. J. & Oberg, C. J. 1999. Deconstructing Mozzarella. *Dairy Industries*  
 427 *International*. 64 7 23-26

428 McMahon, D. J., Oberg, C. J. & McManus, W. 1993. Functionality of Mozzarella cheese.  
 429 *Dairy Industry Association of Australia, 8<sup>th</sup> Annual Conference, Melbourne, Australia*.

430 Pan, K. & Zhong, Q. 2015 Amyloid-like fibrils formed from intrinsically disordered caseins:  
 431 physicochemical and nanomechanical properties. *Soft Matter* 11, 5898-5904

432 Rowney, M., Roupas, P., Hickey, M. W. & Everett, D. W. 1999. Factors affecting the  
 433 functionality of mozzarella cheese. *Australian Journal of Dairy Technology*. 54 2 94-103.

434 Rowney, M., Roupas, P., Hickey, M. W. & Everett, D. W. 1998. Milkfat structure and free oil  
 435 in Mozzarella cheese. *Australian Journal of Dairy Technology*. 53 2 110

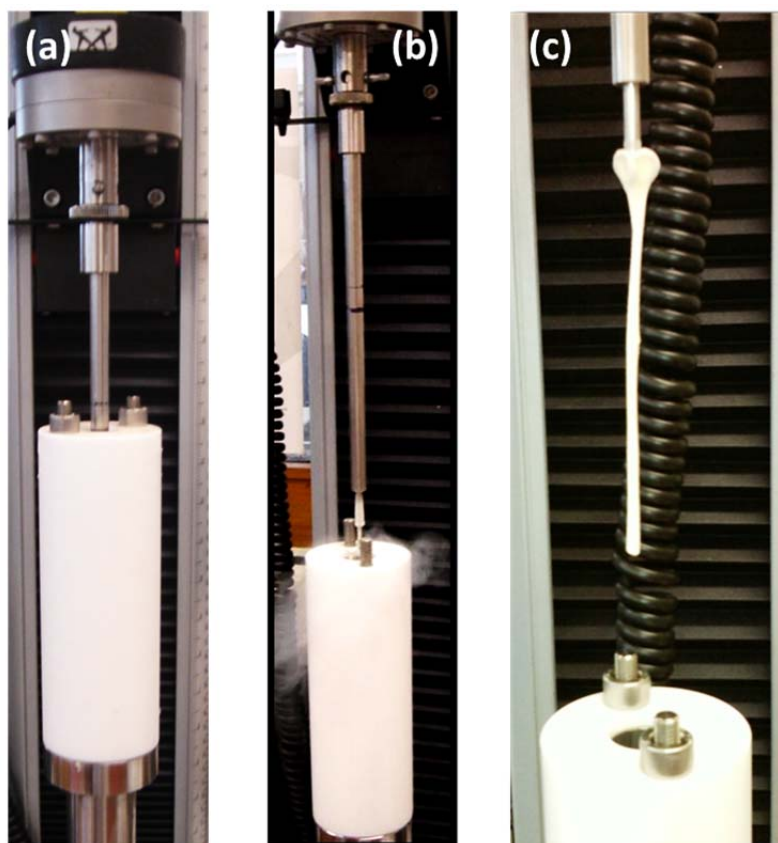
436 Walstra, P., Wouters, J. & Geurts, T. 2006. *Dairy Science and Technology*. Boca Raton:  
 437 CRC Press/Taylor & Francis.

438 Wang, Y. C., Muthukumarappan, K., Ak, M. M & Gunasekaran, S. 1998. A device for  
 439 evaluating melt/flow characteristics of cheeses. *Journal of Texture Studies*. 29 43-55.

440

441 Figures

442



443

444 Figure 1: Extraction of sample stretched to 100mm and quenched.

445

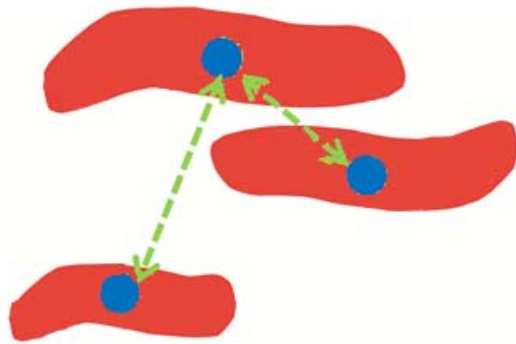
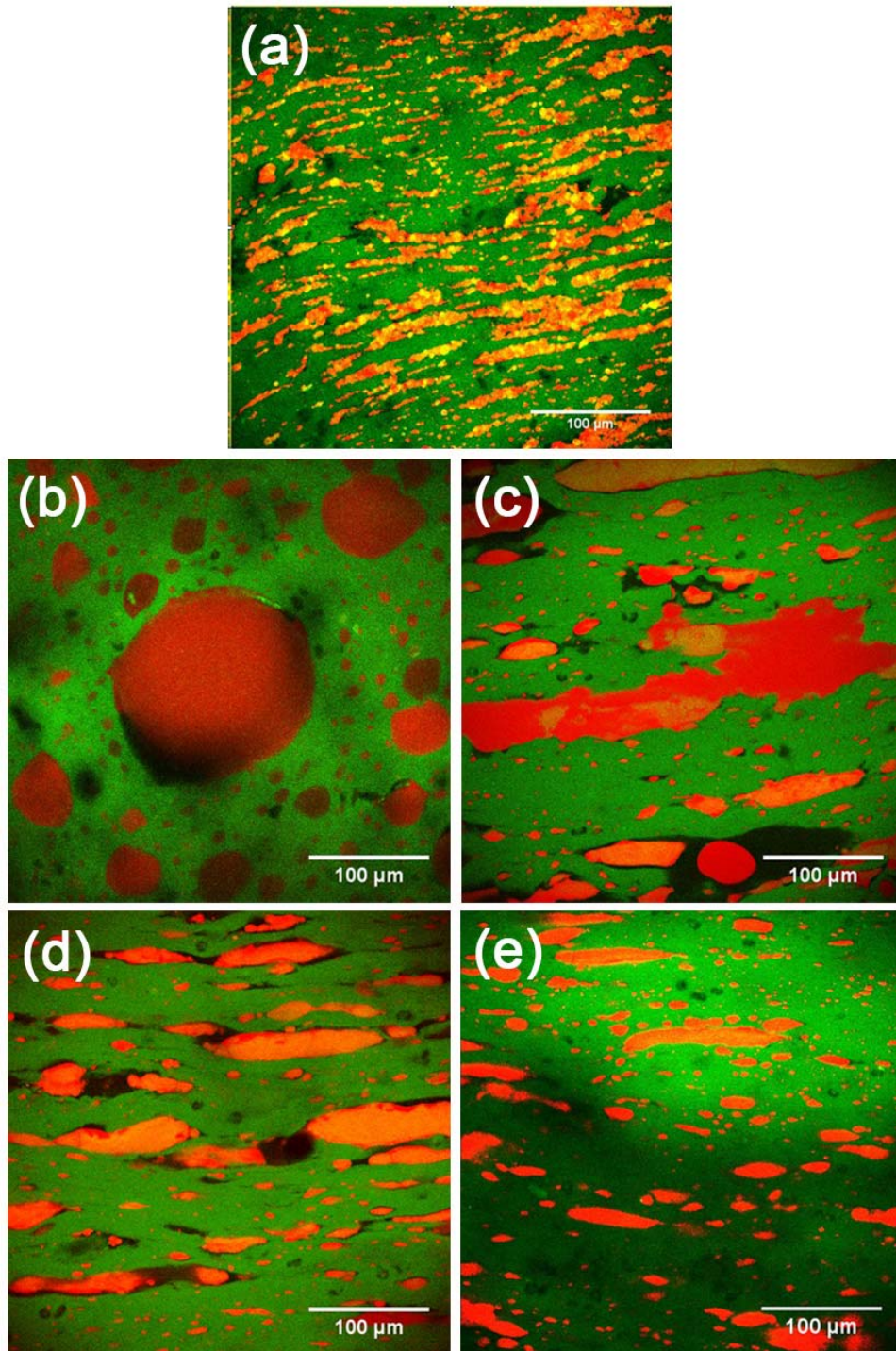


Figure 2: Schematic illustration demonstrating measurement of minimum distance to neighbouring fat channels. Distance (arrows) between the centres of gravity (circular dot) of each fat channel.



454

455 Figure 3: CLSM images of unmelted, melted and stretched mozzarella in the longitudinal  
 456 axis. (a) Unmelted mozzarella at 4°C; (b) Melted mozzarella at 70°C; (c) mozzarella  
 457 stretched by 280% strain; (d) mozzarella stretched by 580% strain; (e) mozzarella stretched  
 458 by 900% strain. Red = Fat, Green = protein

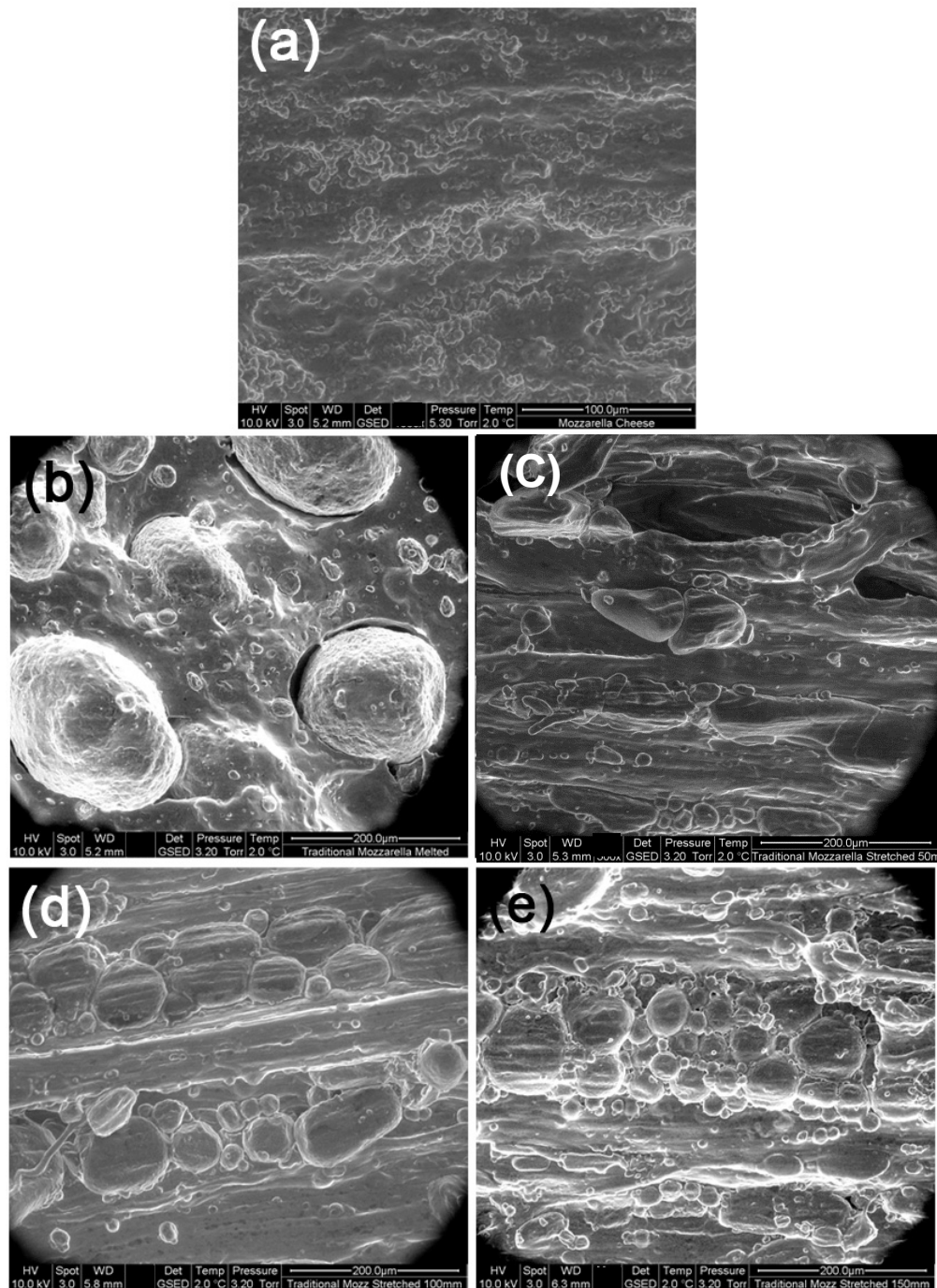
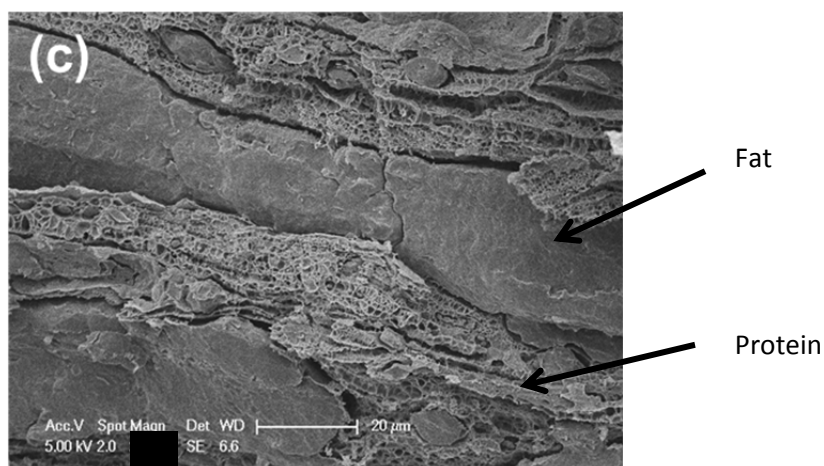
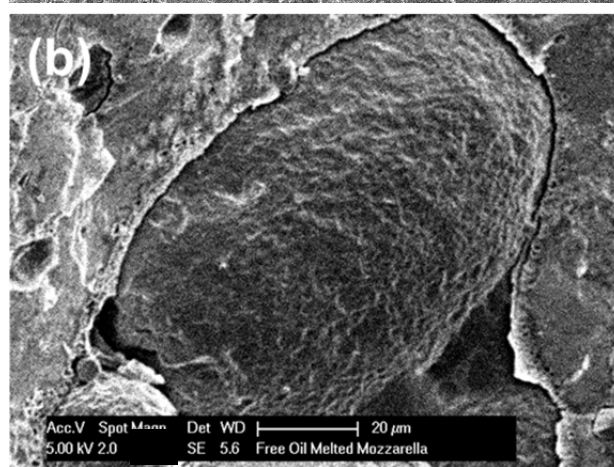
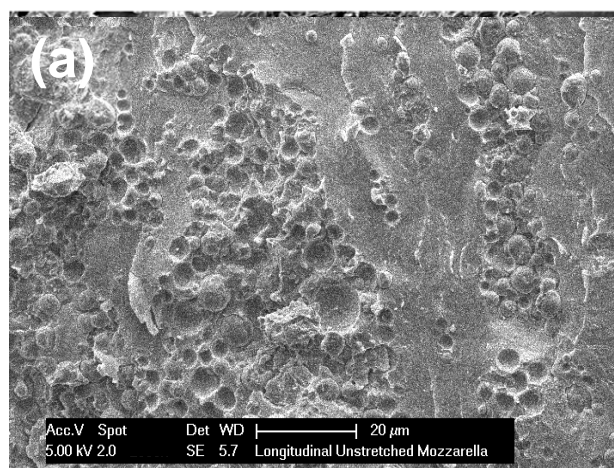


Figure 4: Environmental scanning electron micrographs showing internal microstructure of mozzarella (longitudinal axis) in different states: (a) unmelted mozzarella at 4°C; (b) Melted mozzarella at 70°C; (c) mozzarella stretched by 280% strain; (d) mozzarella stretched by 580% strain; (e) mozzarella stretched by 900% strain.



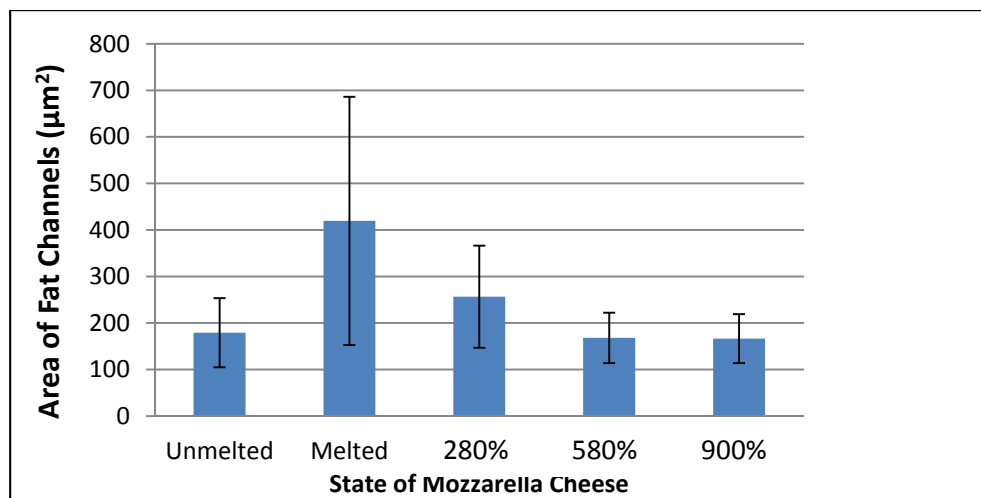


465

466 Figure 5: Cryo scanning electron micrographs showing internal microstructure of mozzarella  
 467 (longitudinal axis) in different states: (a) unmelted mozzarella at 4°C; (b) Melted mozzarella  
 468 at 70°C; (c) mozzarella stretched by 280% strain.

469

470



471

472 Figure 6: Change in individual size of fat channels in unmelted, melted and stretched  
473 mozzarella. Error bars are 95% confidence intervals.

474

475

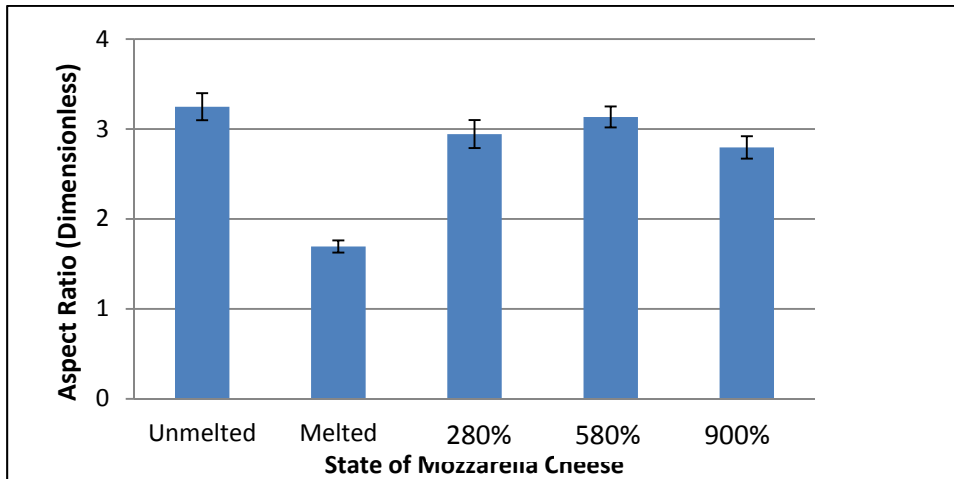


Figure 7: Change in aspect ratio of fat channels in unmelted, melted and stretched mozzarella. Error bars are 95% confidence intervals.

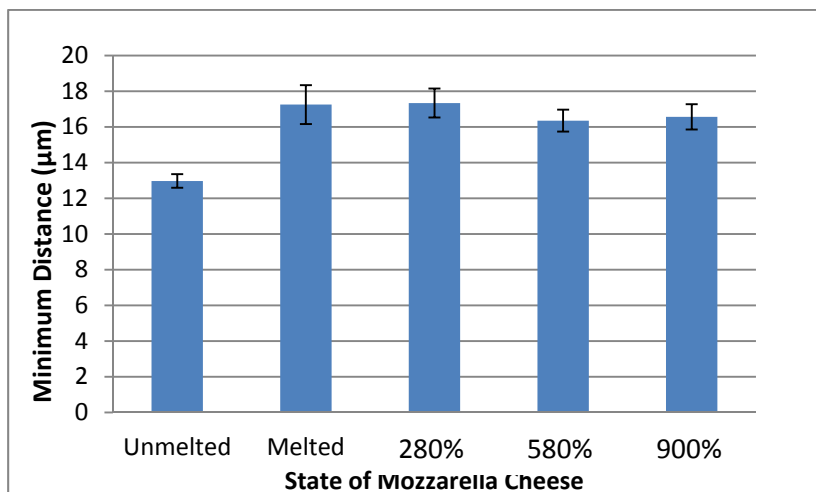
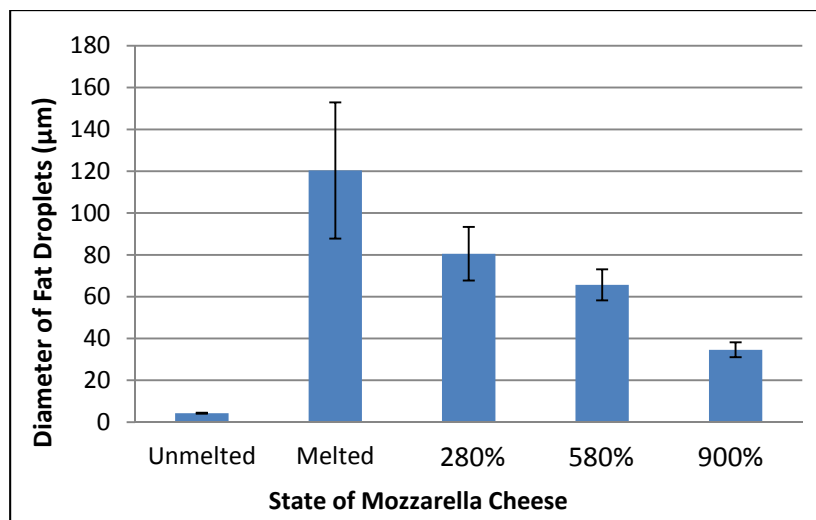


Figure 8: Change in minimum distance between neighbouring fat channels in unmelted, melted and stretched mozzarella. Error bars are 95% confidence intervals.

485



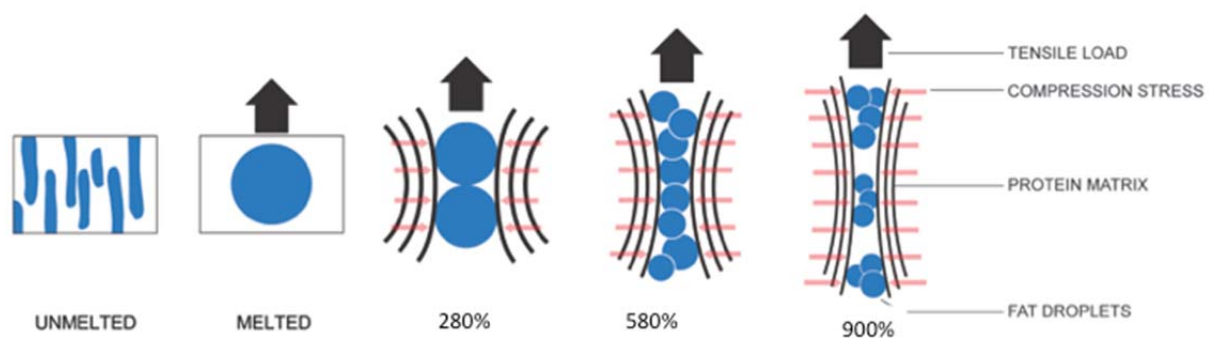
486

487 Figure 9: Change in diameter of individual fat globules and droplets within fat channels in  
488 unmelted, melted and stretched mozzarella. Error bars are 95% confidence intervals.

489

490

491



492

493 Figure 10: Diagram illustrating change in fat structure and distribution of forces in the  
494 unmelted, melted and mozzarella stretched by a strain of 280%, 580% and 900%.

495

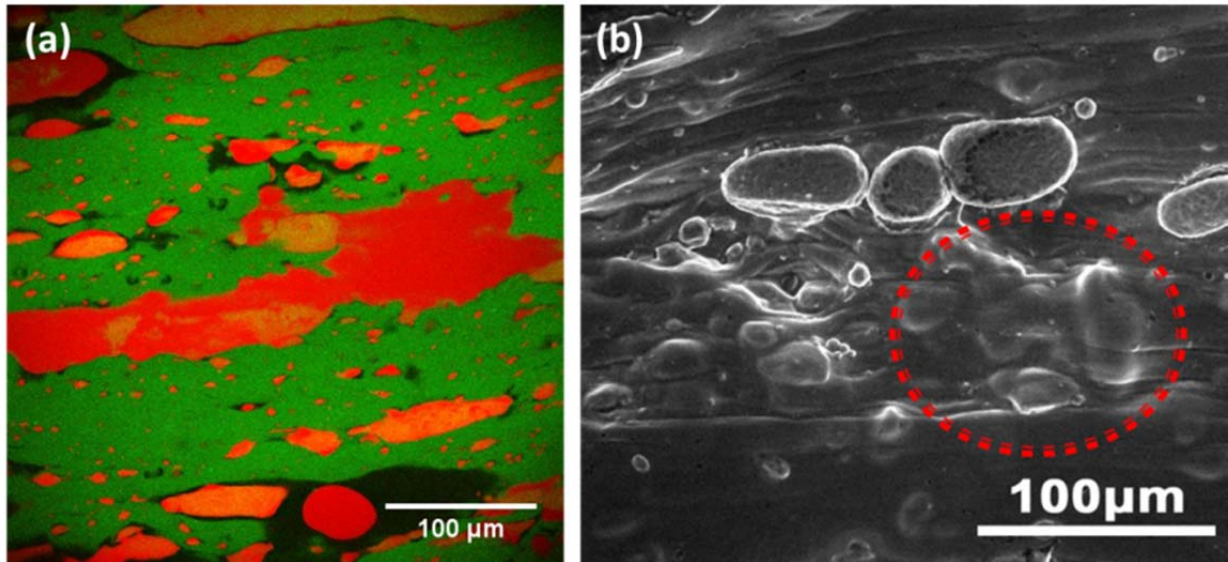


Figure 11: Comparison of image taken across a plane in CLSM and image taken from the surface in ESEM in mozzarella stretched by 280% strain.